PROCEEDINGS OF SPIE

SPIEDigitalLibrary.org/conference-proceedings-of-spie

# First lab results of the WEAVE fibre positioner system

Schallig, Ellen, Lewis, Ian, Dalton, Gavin, Brock, Matthew, Terrett, David, et al.

Ellen Schallig, Ian J. Lewis, Gavin Dalton, Matthew Brock, David Terrett, Don Carlos Abrams, Kevin Middleton, Georgia Bishop, J. Alfonso L. Aguerri, Piercarlo Bonifacio, Esperanza Carrasco Licea, Scott C. Trager, Antonella Vallenari, "First lab results of the WEAVE fibre positioner system," Proc. SPIE 10702, Ground-based and Airborne Instrumentation for Astronomy VII, 107027X (16 July 2018); doi: 10.1117/12.2312703

SPIE.

Event: SPIE Astronomical Telescopes + Instrumentation, 2018, Austin, Texas, United States

# First lab results of the WEAVE fibre positioner system

Ellen Schallig*[a], Ian J. Lewis[a], Gavin Dalton[a,b], Matthew Brock[a], David Terrett[b], Don Carlos Abrams[c], Kevin Middleton[b], Georgia Bishop [b], J. Alfonso L. Aguerri[d], Piercarlo Bonifacio[e], Esperanza Carrasco Licea[f], Scott C. Trager[g], Antonella Vallenari[h]

[a]Dept. of Physics, Keble Road, University of Oxford, OX1 3RH, UK; [b]RAL Space, Science and Technology Facilities Council, Rutherford Appleton Laboratory, Harwell Oxford, OX11 OQX, UK; [c]Isaac Newton Group, 38700 Santa Cruz de La Palma, Spain; [d]Instituto de Astrofisica de Canarias, 38200 La Laguna, Tenerife, Spain; [e]GEPI, Observatiore de Paris, Place Jules Janssen, 92195 Meudon, France; [f]Instituto Nacional de Astrofisica, Optica y Electronica (INAOE), Mexico, [g]Kapteyn Instituut, Rijksuniversiteit Groningen, Postbus 800, 9700 AV Groningen, Netherlands, [h]Osservatorio Astronomico di Padova, INAF, Vicolo Osservatorio 5, 35122, Padova, Italy

## ABSTRACT

WEAVE is the new wide-field spectroscopy facility for the prime focus of the William Herschel Telescope on La Palma in the Canary Islands, Spain. It is a multi-object "pick-and-place" fibre-fed spectrograph with a 960 fibre multiplex behind a new dedicated 2° prime focus corrector. We provide an update on the fibre positioner's technical progress. The hardware has been fully assembled and integrated with its control system for testing. We have made initial calibrations and are starting to move test fibres. In the near future we will dismantle for final modifications and surface anodising, before final reassembly and full fibre installation.

**Keywords:** fibre spectroscopy, WHT, WEAVE, robotic positioners, high multiplex spectroscopy
*ellen.schallig@physics.ox.ac.uk

## 1. INTRODUCTION

The WEAVE spectroscopy facility is the new workhorse for the William Herschel Telescope[1,2]. It consists of a spectrograph system[3], a prime focus corrector, and a fibre positioner. The prime focus corrector provides a field of view of 2 degrees, across a flat focal surface 410 mm in diameter. This focal plane can be populated by up to 960 optical fibres to feed light to the spectrographs, plus 8 coherent fibre bundles feeding an autoguider.

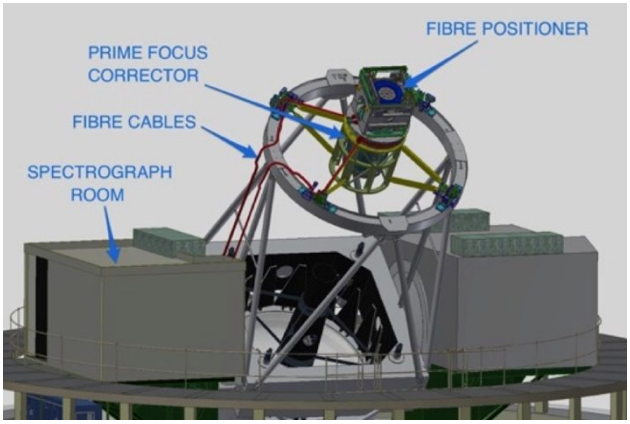


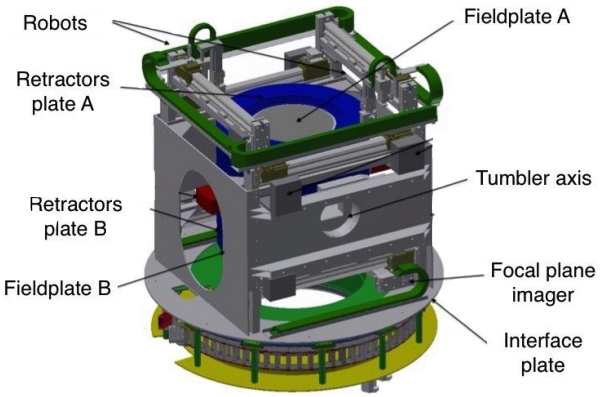


**Figure 1**. *On the left:* overview of the WEAVE instrument. The main components are the prime focus corrector, the spectrograph, and the fibre positioner. Also shown: the fibre cables coming from the positioner and going to the spectrograph. *On the right:* a close-up of the fibre positioner.

Ground-based and Airborne Instrumentation for Astronomy VII, edited by Christopher J. Evans, Luc Simard, Hideki Takami, Proc. of SPIE Vol. 10702, 107027X · © 2018 SPIE · CCC code: 0277-786X/18/$18 · doi: 10.1117/12.2312703

The fibre positioner takes care of the accurate placement of these fibres on the fieldplate. To maximise the efficiency of the instrument, there are two sets of fibres and fieldplates. While one plate is in the focal plane, a pair of fibre-positioning robots can reconfigure the other plate. To move to a new field, the reconfigured plate is tumbled into the focal plane, and the old plate is tumbled to the robots to be reconfigured. The spectrograph and autoguider are also switched to the other set of fibres at this point. Reconfiguring a fibre layout for a new field has to be achieved within about 60 minutes, the length of a typical dwell time on a target field. A breakdown of how this is achieved can be found in Gilbert[4].

There will be three working modes: a MOS (multi-object spectrograph) mode with up to 968 movable fibres per field as explained above, an IFU (integral field unit) mode with 20 movable small IFUs, and a single large IFU mode. The IFUs will be hex packed with 37 fibres in each small IFU and 547 (plus an additional 56 distributed in eight 7-fibre sky bundles) in the LIFU. This paper will deal mainly with the MOS mode, as a bundle of 24 MOS fibres has been manufactured and provided for testing.

In this paper we provide an update on the first lab results of the fibre positioner system. We have built the whole positioner system and populated a few retractors with the test fibres (Section 2). With these fibres we calibrate the gripper optical system (Section 3). To perform repeatability measurements (Section 4) and gantry calibration (Section 5) we also use high-level control software (Section 6).

## 2. RETRACTOR ASSEMBLY

The positioner tumbler assembly is used to switch between two sets of 168 fibre retractors. Each retractor houses six fibres. We have test-assembled four retractors with 24 fibres from a single test fibre bundle[5]. This has allowed us to verify the assembly process for practicality and time required. At a maximum of four retractors per day this task will take almost three months in total. In true time however, it will take longer, as we will do system testing concurrently. The picture below shows the assembled and populated retractor units together with some empty retractor units.

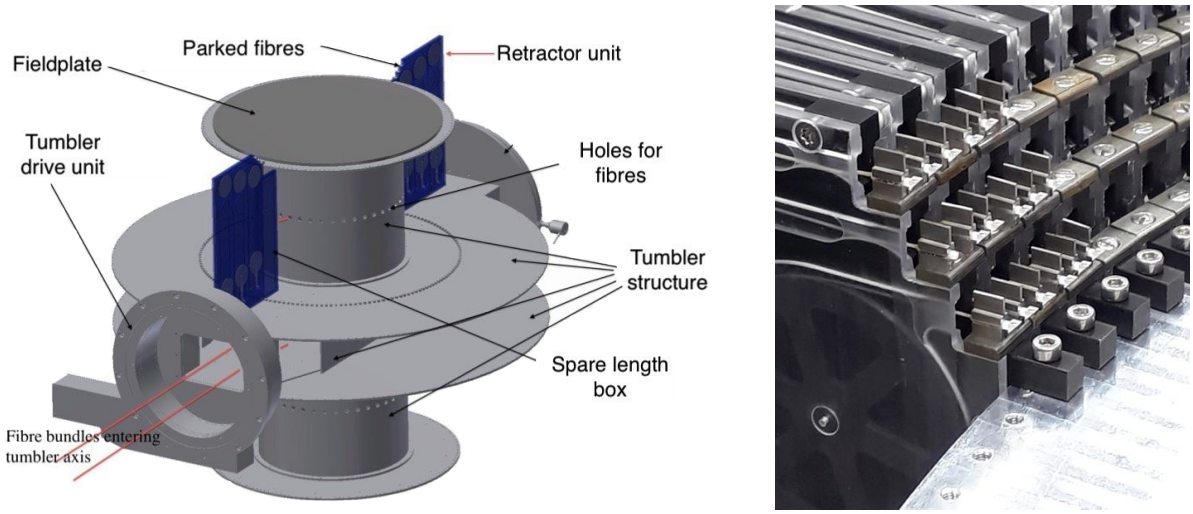


**Figure 2**. *On the left:* the tumbler system. *On the right:* four populated retractors alongside some empty retractors at the edge of the fieldplate.

## 3. GRIPPER OPTICS

Two robots on (x, y, z, θ)-gantries equipped with grippers are able to position the fibres anywhere on the fieldplate. The robots share the x-gantries, which consist of two rails. Each robot moves independently and software ensures that they do not run into each other. Each gripper is mounted below a θ-axis on a z-gantry, which is mounted to a y-gantry. See Figure 3 for an overview, and Schallig et al.[6] for more background information on the gripper units. Each robot has an optical system that is mounted next to the gripper under the θ-axis, and together they form the gripper optical system.

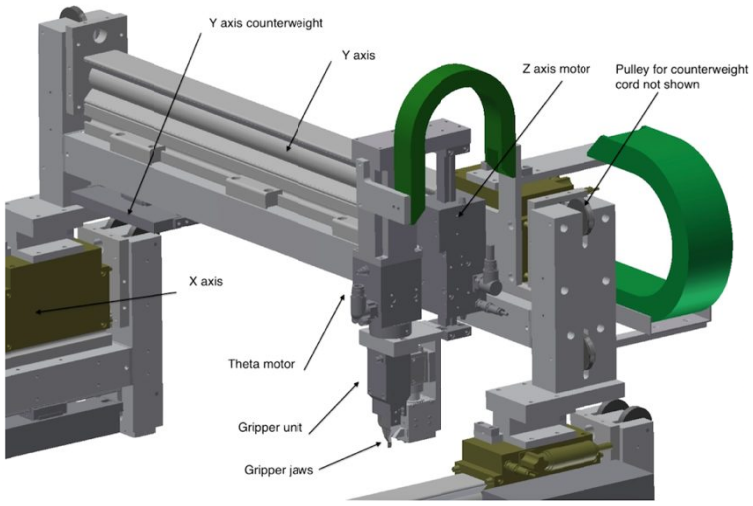


**Figure 3**. Each gripper is mounted on its own (y, z, θ)-axes, and shares the two x-gantries with the other robot.

The optical system has two foci with the same image scale, but in different places. One focus is located close to the rotation centre of the gripper and images a fibre held in the gripper jaws. The second focus images the fieldplate with the gripper raised, as a tool for calibrating fibre locations. Figure 4 shows the setup both as a schematic and the working unit in the lab. The green lines show the two foci.

This setup needs to be calibrated for image scale and rotation centre. A glass distortion target can be imaged to measure the field of view, image scale, and orientation. The pattern has 125 μm spacing and 62.5 μm dot diameter. The image scale is close to the quoted 4.5 μm per pixel of the camera, but we are still investigating whether the nominal 1:1 reimaging optical system has introduced local variations.

The rotation centre is found by imaging a stationary backlit fibre with different gripper orientations. The locus of these images describes a circle, the centre of which is the mechanical rotation axis. This axis is the reference for positioning fibres. We then use the image scale to convert this pixel location to a position expressed in robot coordinates.

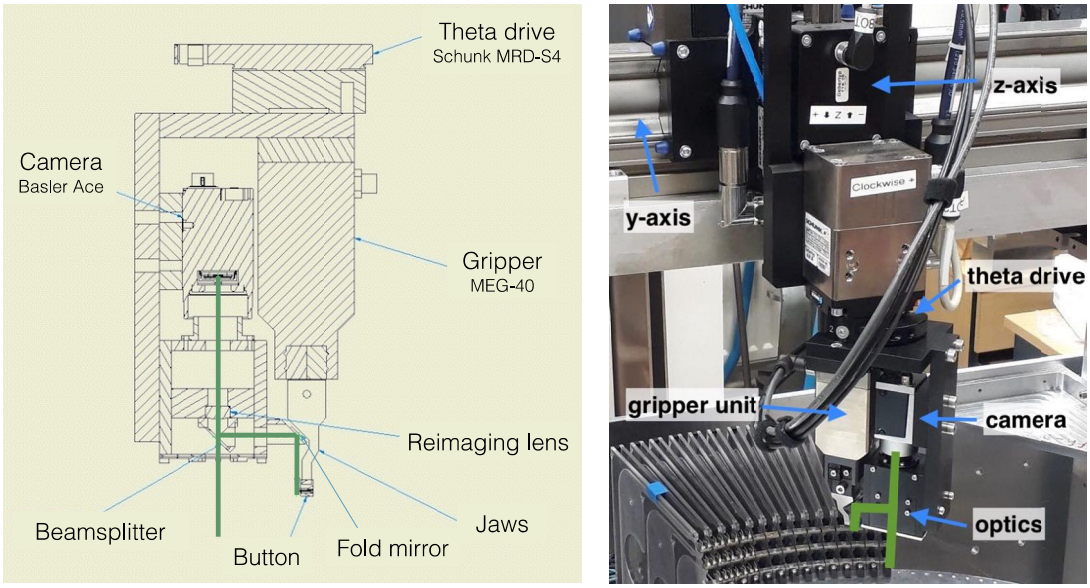


**Figure 4**. The gripper and camera unit. *On the left:* a schematic display. *On the right:* the actual unit in the lab. In both images the green lines denote the two paths the light can travel into the camera.

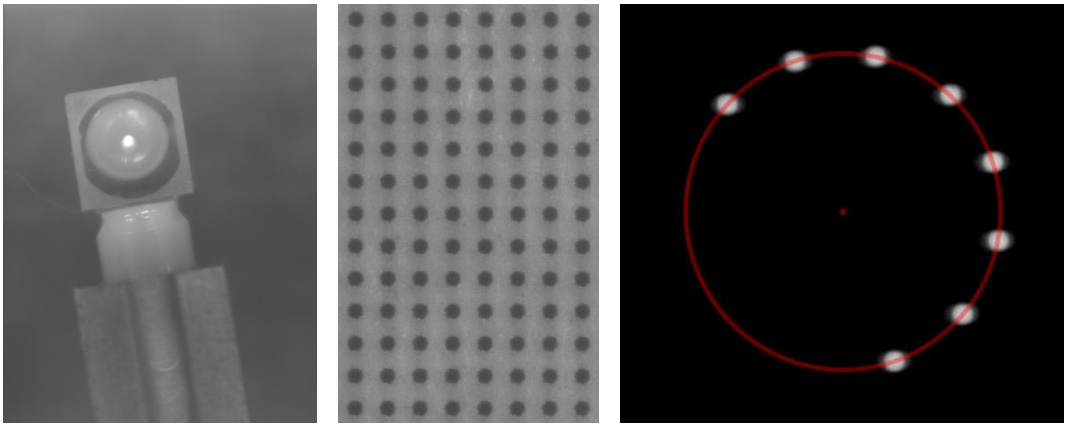

**Figure 5**. *On the left:* a backlit fibre button as seen by the plate-viewing focus. In normal operation only the spot in the prism is visible. *In the middle:* a close-up of the glass distortion target, with 62.5 µm dot size and 125 µm spacing. *On the right:* the result of rotating the gripper and camera unit about its axis and imaging the fibre. Each image represents a 30-degree rotation.

## 4. REPEATABILITY OF ROBOT AXES

We can test the repeatability of the robot gantries by measuring a reference point 50 or 100 times with the gripper optical system, moving away from the point in between measurements. This reference point is a stationary, backlit fibre on the fieldplate. Its position is the centroid of the fibre within the image, in pixel coordinates, when the robot has returned to the same position. Repeating this measurement between gantry movements should yield the same result. To make sure that the move has completely finished, each measurement is taken 2 seconds after the robots have reported the end of the move.

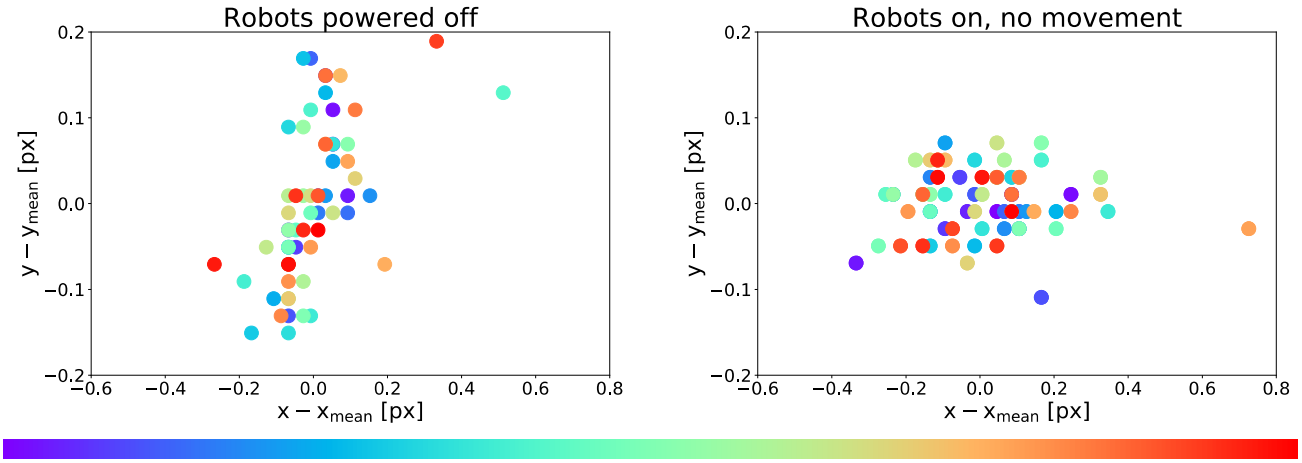


**Figure 6**. The gripper optical system measuring a stationary fibre, 50 data points each. *On the left:* the robot motors are completely switched off. *On the right:* the robot motors are switched on, but there is no movement away from the fibre in between measurements. The colours denote a time series to check for temporal effects, with blue the early measurements and red the later ones.

In Figure 6, both graphs show the repeatability of the system when the robots have not moved in between the measurements. In the first graph the whole system is powered off and the brakes are on, so gantry movement is physically impossible. There can still be vibrations in the whole system though. In the second graph the robots are on, but no commands are given to move anywhere. The gantries operate as a closed-loop positioning system and will stay as

close as possible to the given position. In both graphs we can see structure; the measurements are lining up horizontally and vertically. This is because the centroiding algorithm[4] has a variable resolution, and here we reach the limit of the resolution we chose. It is clear that the spread is very small in both cases, smaller than ±0.5 px for almost all points in x, and ±0.2 px in y, and this provides a good starting point for the tests with movement included.

The first graph in Figure 7 shows the repeatability when moving away and back 100 mm in both x and y, with the colours again denoting a time series to check for temporal effects. There is no strong shift of position with time. The repeatability stays within ±1.5 px. The second graph shows the same for a movement in z of 22 mm, and shows significant non-repeatability in the measured position, with a strong correlation between x and y. This seems to be connected to pitch and yaw errors in the linear motor. The central bulge looks to be about the same size as the total spread in the graph on the left. In consultation with the manufacturers, we are investigating adjusting the mechanical pre-load to reduce the pitch and yaw errors.

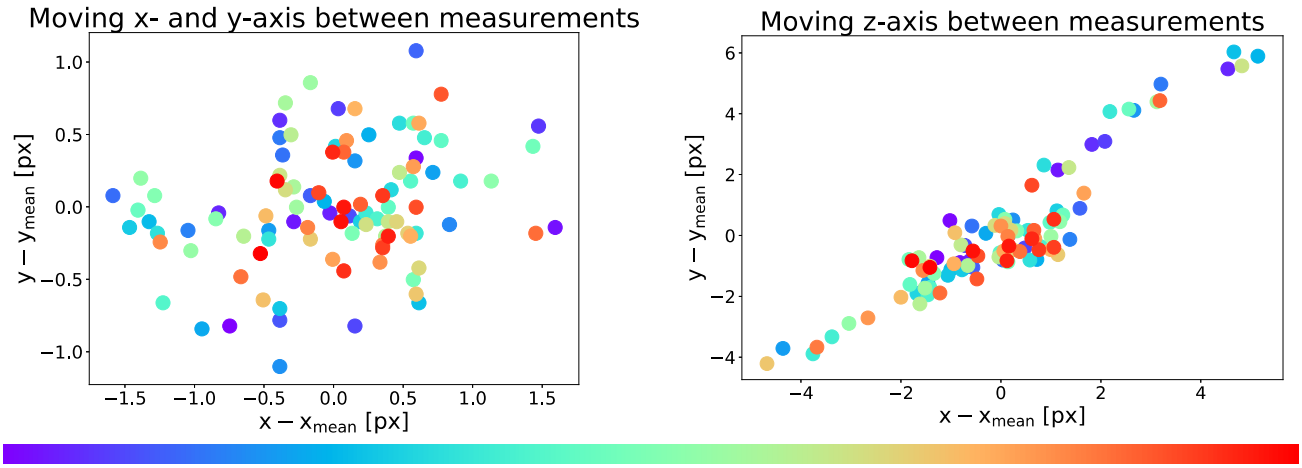


**Figure 7**. Effect of moving the gripper optical system away from and back to a stationary reference point, 100 data points each. *On the left:* movement in the x- and y-direction. *On the right:* movement in the z-direction. The colours denote a time series to check for temporal effects, with blue the early measurements and red the later ones.

## 5. GANTRY CALIBRATION

Although the encoding on the motors is very accurate, we need to calibrate the relationship between the x- and y-axis for each robot. To do this, we measure a fixed reference grid with the gripper optical system, which is situated on the gantries. This reference grid is machined into the surface of each Invar fieldplate and consists of approximately 350 points in a 20 mm grid. These holes are 0.5 mm in size and painted black, to keep the plate smooth and make the contrast between the grid points and the rest of the plate large enough for the optical system.

We have used a dummy aluminium fieldplate with a partially painted grid to prototype this process. The aluminium plate is lighter in colour than the Invar one, and so makes it easier to see the black grid points, but a test with a small piece of Invar and paint showed that the contrast is still large enough.

By comparing these measured positions and the expected positions of the grid, we can determine the gantries' x- and y-offsets, x- and y-scales, rotational alignment, and shear. We use the SLALIB library[7] to compare the two datasets and generate a series of residuals, which are then used to estimate the straightness of each robot axis.

To take images of all the grid points, we find the location in robot coordinates where the central grid point is imaged roughly in the centre of the camera chip. Then from there we take 20 mm increments in the x- and y-direction, until the entire grid is covered. These robot positions we also take as the ‘expected’ grid, for ease of calculation.

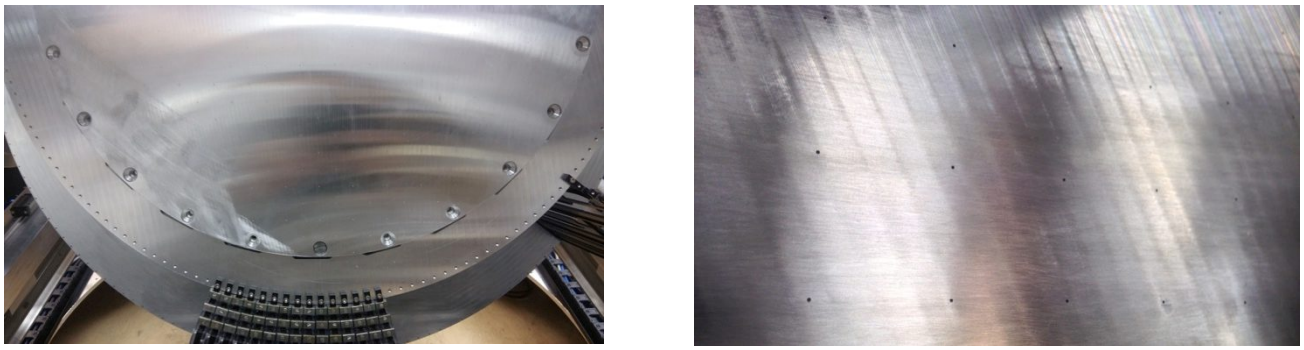

**Figure 8**. *On the left:* the aluminium fieldplate on the tumbler as seen from above, with a few empty retractors on the side. *On the right:* a close-up of the grid machined into the fieldplate. Each point is 0.5 mm wide, and the ones visible here are filled with black paint and lightly sanded.

With the same centroiding algorithm as in Section 4, we then find the location of each grid point on the image, in pixel coordinates. Using a pixel scale of 4.5 μm per pixel, we convert this to a measurement we can then add to the robot coordinates. This is our 'measured' grid. The large offset of several mm between the expected and measured grid is artificially made smaller in the code to prevent this from overwhelming our results. The reported numbers below for the offset include this shift separately.

The first image below in Figure 9 shows the raw residuals, with only the offset mentioned above applied (2.1 mm in x, 2.9 mm in y). A strong shear is visible. The second image shows the residuals after removing the shear (−0.22°), rotation (−0.056°), offset (−0.03098 + 2.9 mm in x, −0.00779 + 2.1 mm in y), and scale (0.99993 in x, 1.00007 in y). These much smaller residuals are used to estimate the straightness of each robot's x- and y-axes.

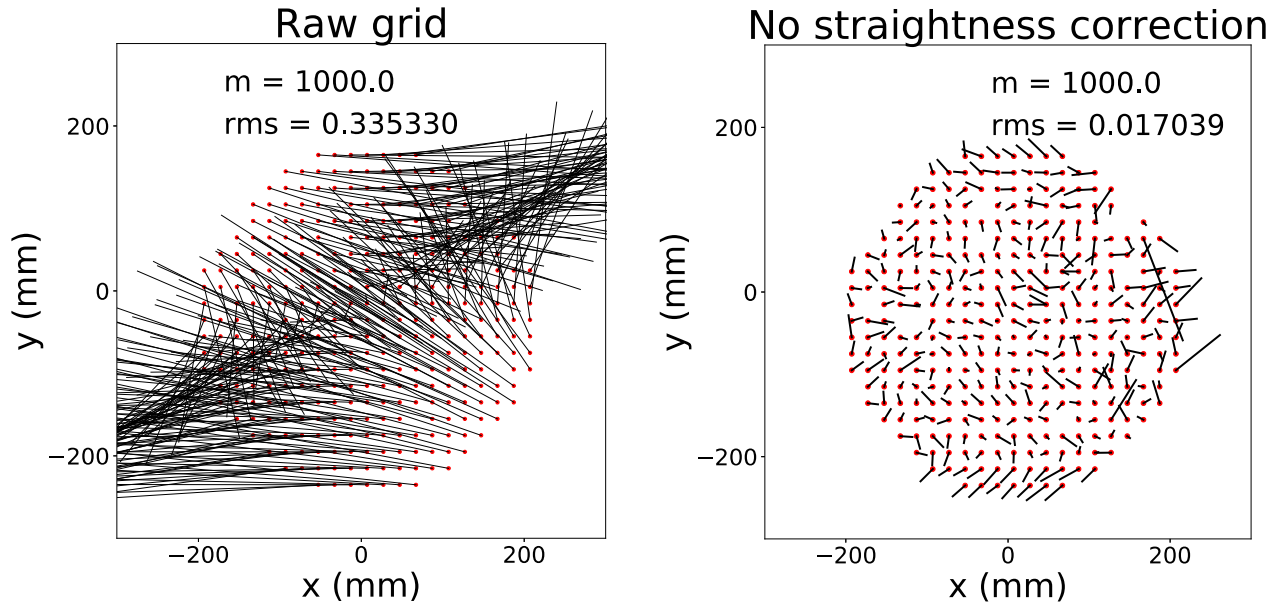


**Figure 9**. The measured grid on a fieldplate. The red dots represent the 'expected' grid; the black lines represent vectors from the expected value to the measured value. The length of each line is multiplied by 1000, to make them easily visible. The quoted rms is in mm. *On the left:* the raw grid shows large residuals, of which shear is the main component. This is due to a non-perpendicularity of the x- and y-axes that the optical system moves on. *On the right:* the remaining residuals when rotation, shear, offset, and scale are taken out.

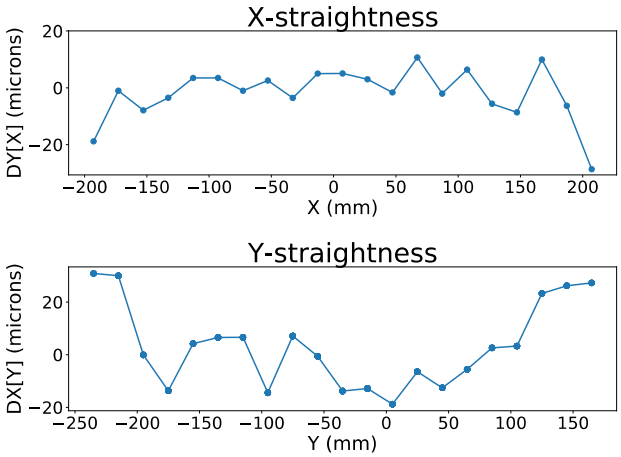


**Figure 10**. An example of the straightness of each axis. These are preliminary values only valid for the initial assembly of the positioner. These will be recalibrated after the full reassembly. The non-straightness is mainly due to the clamping of the robot axes to their support rails and flexure due to gravity.

After removing the model fit from the measurements, we average the y-residuals as a function of the x-position to estimate the straightness of the x-axis. We repeat this for the average x-residuals as a function of y-position to estimate the straightness in the y-axis. This is shown in Figure 10. With these straightness values, we can remove any last systematic errors, and only random errors (e.g. in grid machining precision) should be left over.

## 6. SOFTWARE TESTING

A suite of software has been written to provide low-level and high-level control of the robot. We have tested the long-term reliability of the low-level control (the PLC), and of the software as a whole. The communication is reliable and robust. The interface will need a few upgrades, most importantly temperature monitoring of the motors, additional status gathering (better logs), and an ability to switch the robots to different preset speeds.

We have also tested a piece of software called DELTA[8], which instructs the robots how to physically reconfigure a field from one configuration to the other. It tells each robot which fibre to pick up next and where to move to, ensuring that the fibres will not get tangled and the robots do not run into each other or into the fieldplate. We have tested all the movements (without the fibres), and we see that fields are reconfigured without any problems.

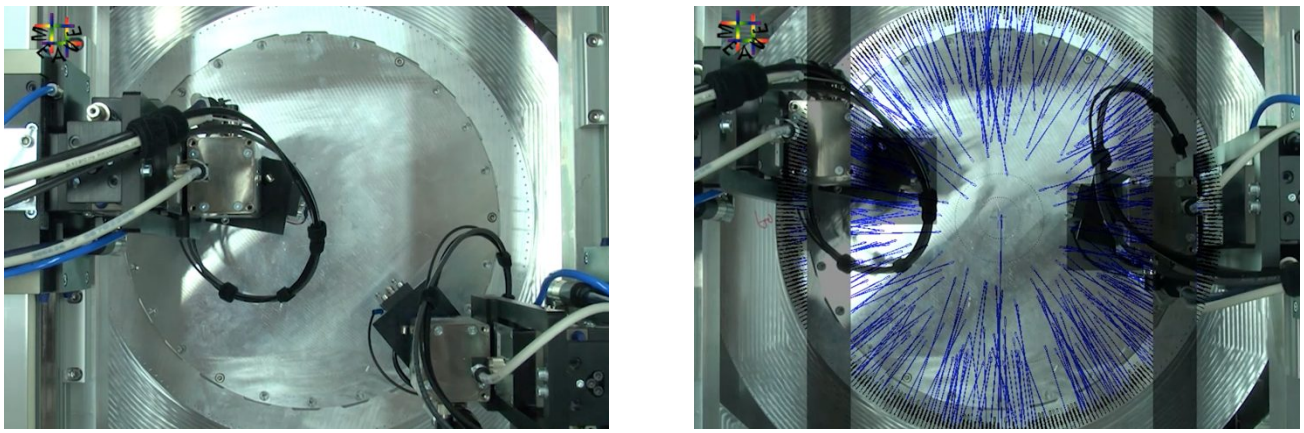

**Figure 11**. The two robots are reconfiguring a field. There are no physical fibres present. *On the left:* top-down view of just the robots. *On the right:* top-down view of the robots with a software mimic of the fibres overlaid. The partial reconfiguration is made visible this way.

## 7. FUTURE WORK

In the immediate future we will dismantle the whole positioner to make some final modifications and to anodise key parts. This is to make them more resistant against corrosion and to prevent stray light bouncing around the structure and entering the fibres. Then we will build up the positioner carefully, ensuring that all parts are properly secured and that the key parts are positioned within tolerance. We will use a combination of a Faro tracker, Faro arm, and several precision dial gauges for this.

With the final Invar fieldplates that are machined to a higher standard than the prototype aluminium fieldplate, it should be easier to get good measurements for each grid point. This should make the centroiding more reliable and give a better result of where the grid points actually are. This corrected grid can then serve as the expected grid for later grid measurements when the positioner is on the telescope and is influenced by changing gravity vectors and other factors.

## 8. SUMMARY

We are in the final stages of assembling the WEAVE fibre positioner, commissioning its low-level PLC control system and developing algorithms to assess its overall performance. We have fully integrated the hardware with the high-level control software, and have tested all key functionality requirements. We have also identified a major issue in the performance of one of the robot axes (z), and we are in the process of fixing this.

## REFERENCES


[1] Dalton et al., “Final design and progress of WEAVE: the next generation wide-field spectroscopy facility for the William Herschel Telescope”, Proc. SPIE 9908, Ground-based and Airborne Instrumentation for Astronomy VI, 99081G (4 August 2016); doi: 10.1117/12.2231078

[2] Dalton et al., "Construction progress of WEAVE: the next generation wide-field spectroscopy facility for the William Herschel telescope", 10702-47, these proceedings (2018)

[3] Stuik et al., “Integration and testing of the WEAVE spectrograph”, 10702-275, these proceedings (2018)

[4] Gilbert, J., “New developments in robotic fibre positioning for astronomical multi-object spectroscopy,” Ph.D. dissertation, University of Oxford, 2016

[5] Sayède et al., “First results of tests on the WEAVE fibres”, Proc. SPIE 9912, Advances in Optical and Mechanical Technologies for Telescopes and Instrumentation II, 991220 (22 July 2016); doi: 10.1117/12.2231170

[6] Schallig et al., “Developments in fibre-positioning technology for the WEAVE instrument at the William Herschel Telescope”, Proc. SPIE 9908, Ground-based and Airborne Instrumentation for Astronomy VI, 99087U (9 August 2016); doi: 10.1117/12.2231626

[7] P.T. Wallace, “The SLALIB Library”, ASP Conference Series Vol. 61 (1994)

[8] Terrett et al., “Fibre positioning algorithms for the WEAVE spectrograph”, Proc. SPIE 9152, Software and Cyberinfrastructure for Astronomy III, 91520P (18 July 2014); doi: 10.1117/12.2055844